Front. Phys., 2014, 9(2): 210–218
DOI 10.1007/s11467-013-0398-5

RESEARCH ARTICLE

First-principles study on the structure, electronic and magnetic properties of $HoSi_n$ (n = 1–12, 20) clusters

Tai-Gang Liu[1,*], **Wen-Qing Zhang**[2], **Yan-Li Li**[3,†]

[1] *School of Life Science and Technology, Xinxiang Medical University, Xinxiang 453003, China*
[2] *School of Mechanics and Electronics, Henan Institute of Science and Technology, Xinxiang 453003, China*
[3] *Department of Physics, Wuhan University of Technology, Wuhan 430070, China*
*Corresponding authors. E-mail: *liutg@xxmu.edu.cn, †liyanli128@163.com*
Received June 3, 2013; accepted August 25, 2013

The structure, electronic and magnetic properties of $HoSi_n (n = 1-12, 20)$ clusters have been widely investigated by first-principles calculation method based on density functional theory (DFT). From our calculation results, we find that for $HoSi_n (n = 1-12)$ clusters except $n = 7, 10$, the most stable structures are a replacement of Si atom in the corresponding pure Si_{n+1} clusters by Ho atom. The doping of Ho atom makes the stability of Si clusters enhance remarkably, and $HoSi_n (n = 2, 5, 8, 11)$ clusters are more stable than their neighboring clusters. The magnetic moment of Ho atom in $HoSi_n (n = 1-12, 20)$ clusters mainly comes from $4f$ electron of Ho, and never quenches.

Keywords structure, stability, electronic and magnetic properties, $HoSi_n$ cluster

PACS numbers 36.40.Cg, 36.40.Qv, 73.22.-f, 31.15.Ew

Frontiers of Physics

1 Introduction

During the last two decades, transition metal (TM)-doped silicon clusters have aroused enormous interest, which starts from their applications in the semiconductor industry. What's more, the finding that the properties of silicon clusters can be greatly changed after the addition of "impurity" atoms makes researchers interested. Because the TM atoms can saturate the dangling bonds on the surface of Si clusters [1–4], which stabilizes the Si cages. In experiment, Beck pioneered the synthesis of $TMSi_n$ (TM = Cr, Mo, and W) clusters [5, 6] by the laser vaporization supersonic expansion technique, and found that Si clusters doped with TM atoms were more stable compared with pure Si clusters of the same size. Afterwards, Si clusters encapsulated with TM atoms were investigated extensively both in experiment [7–9] and theory [10–17]. The results demonstrated that TM atoms with unpaired d electron stabilize Si cages by placing them inside $TMSi_n$ clusters. Therefore, $TMSi_n$ clusters can play a role of building blocks for cluster-assembled materials, and exhibit novel magnetic, electronic and optical properties etc. However, abundant evidence shows that the d orbitals of the endohedral TM atoms have strong interaction with the sp-orbitals of Si atoms, which leads to the quenching of magnetic moments of TM atoms [18–22]. The introduction of endohedrally rare earth (RE) atoms into Si clusters rather than TM atoms has been seen as a more advanced approach, because the electron residing in the more localized f orbitals of RE atoms hardly participates in bonding. As a result, magnetic moments of $RESi_n$ clusters can often be retained.

Presently, many efforts have been focused on the Si clusters doped with RE atoms. In experiment, Ohara *et al.* [23, 24] investigated the geometric and the electronic structures of $TbSi_n (6 \leqslant n \leqslant 16)$ clusters using photoelectron spectroscopy and chemical-probe method. They found that Tb atom is encapsulated inside the $Si_n (n \geqslant 10)$ cage. Bowen *et al.* studied photoelectron spectroscopic of $EuSi_n^- (3 \leqslant n \leqslant 17)$ [25] and $HoSi_n^-$ [26] clusters. They speculated that $EuSi_n$ and $HoSi_n$ clusters might keep a large portion of their magnetic moments, because Eu and Ho f electrons are involved limitedly in bonding with their surroundings, such as a Si cage. Nakajima and co-workers [27] investigated the adsorption reactivity of anionic $HoSi_n^-$ and the results suggested that the encapsulation of Ho is still incomplete when the size of the Si cage swells to 16 atoms. In theory, the structure and the electronic properties of $RESi_n$ clusters were studied by DFT method [28, 29]. More-

over, Kumar *et al.* [30] studied the $RESi_{20}^{\circ/-}$ (RE=La, Ac, Sm, Gd, Tm, Ce, Pa, Pu, Th, Np, Pm) clusters, which suggested that $SmSi_{20}$, $TmSi_{20}$, $PaSi_{20}$, $PuSi_{20}$, and $GdSi_{20}^{-}$ retain significant magnetic moments in the ground states. Additionally, Liu *et al.* [31] investigated $EuSi_{20}$ fullerene and found that the Eu atom has a large magnetic moment of nearly $7\mu_B$. In this aspect, our research group also carried out some calculations and found that $RESi_n$ (RE=Eu, Gd)clusters retain high magnetic moments [32, 33]. Hence, exploring these clusters, building blocks of silicon-based and cluster-assembled materials, which may show novel magnetic properties, is interesting. Although some research has been done on $RESi_n$ clusters, there is no systematic and theoretical investigation on $HoSi_n$ so far. So it is very necessary to analyze the physical properties of the Ho-doped Si clusters, such as the growth behavior and the size-dependent evolution.

In this paper, we report $HoSi_n$ clusters by considering diverse isomers. The relative stabilities, the electronic and the magnetic properties of $HoSi_n$ clusters are calculated by using first-principles method based on DFT.

2 Computational details

Our calculations are on the basis of DFT, which is implemented in the DMOL3 package [34, 35]. We use the generalized gradient approximation (GGA) with the PW91 function to deal with the exchange–correlation interaction. The convergence criterion is 10^{-6} Hartree on the total energy. As for charge and spin, the density mixing criteria are 0.2 and 0.5, respectively. In order to speed up convergence, we use the Direct Inversion in an Iterative Subspace (DIIS) approach. We also apply a 0.005 Hartree of smearing to the molecular orbital occupation. During the geometry optimization, the convergence thresholds of the forces, displacement and energy change are 0.002 Hartree/Å, 0.005 Å and 10^{-5} Hartree, respectively. We evaluate the on-site charges by Mulliken population analysis. Relativistic effects are also in our consideration. Spin-unrestricted calculations along with the effective core potentials (ECPs) [36, 37], and a basis set composed of double numerical basis ($4f$ and $6s$) with polarized function ($6p$) are conducted.

We calculate harmonic vibrational frequencies for the promising stationary points from a direct structure optimization. If an imaginary vibrational mode is found, we can carry out a relaxation along coordinates of imaginary vibrational mode until the true local minimum is achieved. Thus, the isomers of each cluster are certainly the local minima. However, it is challengeable for us to determine the global minimum structures with the increase of cluster size. According to the available results [38–41], we firstly optimize equilibrium geometries of pure $Si_n (n = 2–13)$ clusters so as to find the most stable geometries of $HoSi_n$ clusters. Then, a Ho atom is placed at various adsorption or substitutional positions: i.e., Ho-capped, Ho-substituted, Ho-concaved patterns along with Si-capped pattern to find the low-lying isomers of $HoSi_n$. Additionally, we optimize the structures of $HoSi_n$ clusters with high symmetry and refer to the configurations of $LuSi_n$ [28], $YbSi_n$ [29], $LaSi_n$ [42], $EuSi_{20}$ [31], $RESi_{20}^{\circ/-}$ [30] clusters.

3 Results and discussion

3.1 Structures of $HoSi_n$

The obtained ground state and the low-lying structures of $HoSi_n$ clusters are shown in Figs. 1–2. The ground state structures of Si_n clusters are also plotted for comparison. Our calculation results are in perfect accordance with the available results [38–41].

For the clusters with $n \leqslant 3$, $HoSi_n$ clusters adopt planar structures as their ground state geometries. The ground state structures of $HoSi_n$ are created by directly substituting the Ho atom for the Si atom in Si_{n+1} clusters. The binding energy per atom and bond length of HoSi dimer are 1.86 eV and 2.843 Å, respectively. The bond lengths for the two Ho–Si bonds and the one Si–Si bond for $HoSi_2$ (Fig. 1, 2a) are 2.784 Å and 2.186 Å, respectively. The linear chain 2b with $D_{\infty h}$ is higher in energy than 2a by 2.72 eV. For $HoSi_3$, the lowest-energy structure 3a is a planar rhombus (C_{2v}) and the energy of the three-dimensional metastable structure 3b is higher than 3a by 0.85 eV.

As the size of cluster increases, 3D configurations prevail in the ground-state structures of $HoSi_n$ clusters. Our calculation results indicate that the most stable structure of $HoSi_4$ (Fig. 1, 4a) is a distorted pyramid with Ho atom on the apex with C_s symmetry. This structure can be seen as Ho atom substituting for a Si atom on the top of $5a_0$ and lower in energy than the other trigonal bipyramid with Ho atom on the triangular base 4b by 0.38 eV. For $HoSi_5$, the most stable isomer 5a with C_s symmetry (Fig. 1, 5a) is one in which a Ho atom gets adsorbed on a bipyramid of Si_5. The metasable isomer 5b with C_s symmetry (Fig. 1, 5b) can be created by substituting Ho atom for Si atom on the vertex of $6a_0$, which is only higher in energy than 5a by 0.1 eV.

The lowest-energy structure of Si_7 is a pentagonal bipyramid with D_{5h} symmetry (Fig. 1, $7a_0$). The

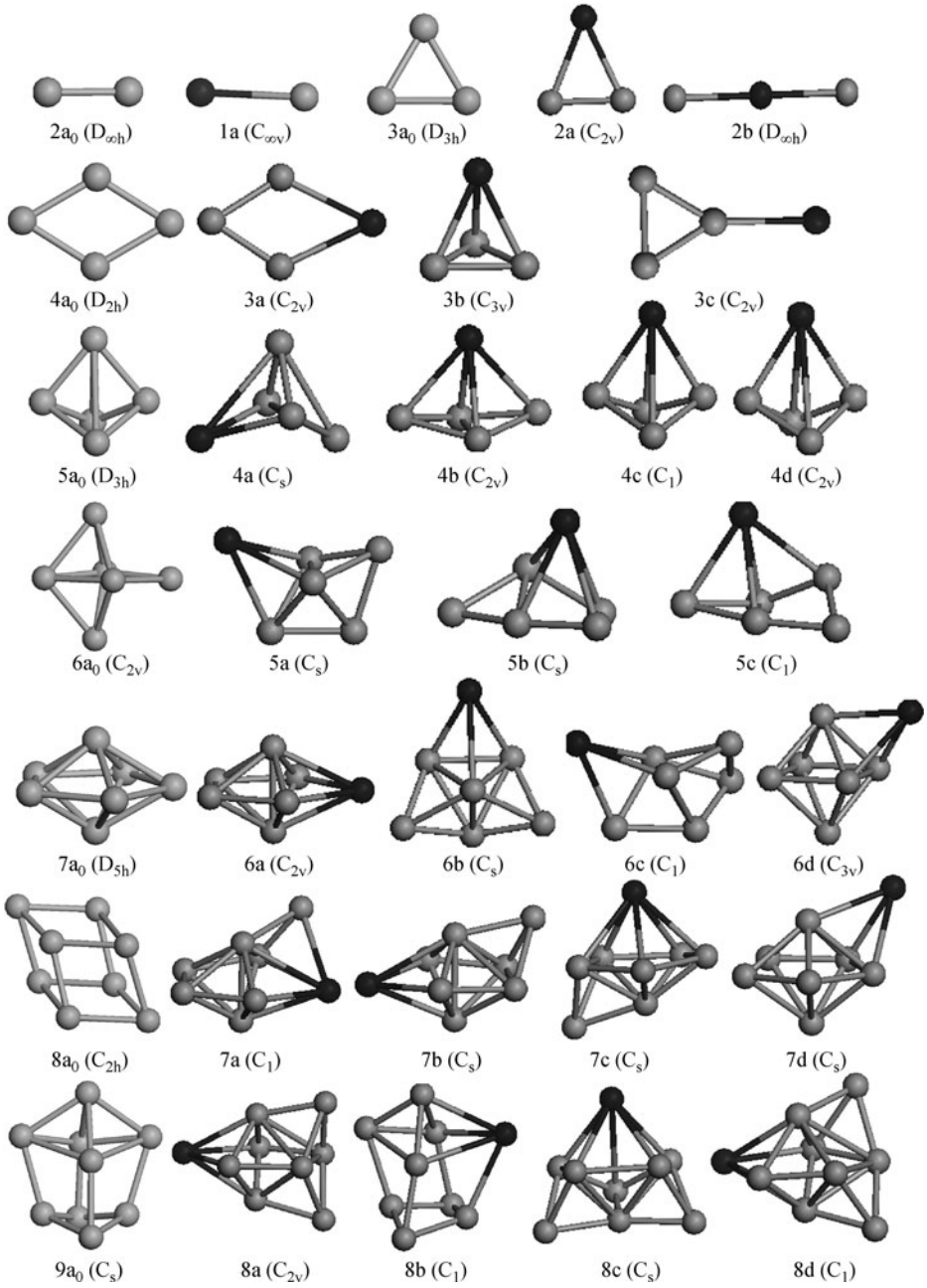

Fig. 1 The lowest-energy and low-lying structures of $HoSi_n$ (n = 1–8) clusters and ground-state structures of Si_{n+1} (n = 1–9) clusters. The Si atoms and Ho atoms are shown in gray ball and dark ball, respectively. The symmetries of $HoSi_n$ clusters are given in the bracket for each size.

ground-state structure of $HoSi_6$ with C_{2v} symmetry (Fig. 1, 6a) can be generated by substituting the Si atom of the ring of the ground state Si_7 isomer, which is well consistent with Ref. [28]. Both of the C_s 6b and C_1 6c isomers can be viewed as capping one Si atom on the most stable $HoSi_5$ isomer at a suitable site, and are higher in energy than 6a by 0.36 eV and 0.57 eV, respectively. Another isomer 6d with C_{3v} symmetry can be regarded as a Ho atom capped on the metastable structure of Si_6.

The most stable structure of Si_8 (Fig. 1, 8a$_0$) is a distorted square prism with C_{2h} symmetry. For $HoSi_7$, the isomers 7a and 7b can be generated by capping one Si atom on the different faces of the most stable $HoSi_6$ isomer, with only 0.01 eV difference in energy. The isomer 7c is higher in energy than 7a by 0.03 eV. Another isomer 7d is obviously created by capping a Ho atom on the face of the ground state for Si_7.

The lowest-energy structure of Si_9 (Fig. 1, 9a$_0$) is a distorted capped cube with C_s symmetry. For $HoSi_8$, the ground-state configuration of $HoSi_8$ (Fig. 1, 8a), a dis-

torted cube with Ho atom on the top (C_{2v}), is viewed as a substitution of Ho atom for Si atom in Si_9. The isomer 8b is also a type of substitution in Si_9, and is higher in energy than 8a by 0.61 eV. The isomer 8c is obtained by adding one Si atom on the surface of $HoSi_7$ 7b cluster. The C_1 8d isomer is a substitution in the metastable structure Si_9.

The ground-state structure of Si_{10} (Fig. 2, $10a_0$) with C_{3v} symmetry is a tri-capped trigonal prism with one Si atom capped on the top face of the prism. The lowest-energy structure of $HoSi_9$ (Fig. 2, 9a), a Si atom capped irregular square prism with a Ho atom on the vertex, can be created by substituting Ho atom for Si atom on the bottom ring of $10a_0$. The metastable structures 9b and 9e can also be viewed as Ho atom substituting for a Si atom on the different vertex of $10a_0$. The other two isomers are generated by capping one Ho atom on the different faces of $9a_0$.

For $HoSi_{10}$, five low energy isomers are obtained as shown in Fig. 2. The ground-state structure of $HoSi_{10}$ (Fig. 2, 10a) with C_s symmetry can be viewed as one Ho atom face-capping on the ground state of Si_{10} (Fig. 2,

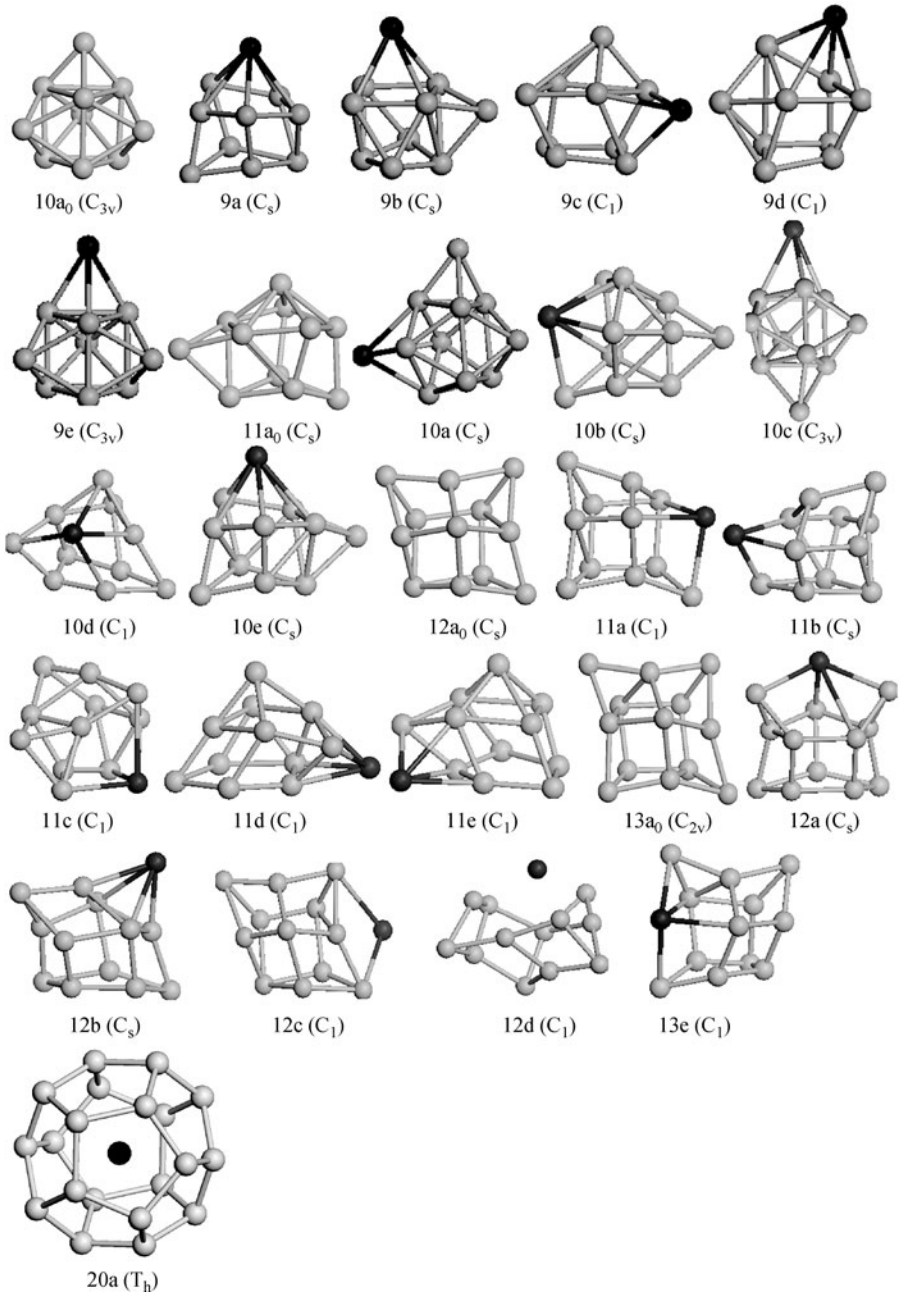

Fig. 2 The lowest-energy and low-lying structures of $HoSi_n$ ($n = 9$–$12, 20$) clusters and ground-state structures of Si_{n+1} ($n = 10$–13) clusters. The Si atoms and Ho atoms are shown in gray ball and dark ball, respectively. The symmetries of $HoSi_n$ clusters are given in the bracket for each size.

10a$_0$). Its energy is 0.085 eV lower than the metastable structure 10b, whose symmetry is the same as 10a. The isomer 10c with C_{3v} symmetry is higher in energy than 10a by 0.18 eV, and it is created by face-capping one Ho atom on the ground state of Si_{11}.

For $HoSi_{11}$, the ground state structure (Fig. 2, 11a) with C_1 symmetry is brought by taking the ground state structure of Si_{12} (Fig. 2, 12a$_0$) and replacing the face Si atom by a Ho atom. The metastable structure 10b is also a type of substitution in Si_{12}, and is higher in energy than 11a by 0.31 eV. The isomer 11c is obtained by capping a Si atom on the face of 10b. The other two isomers are created by capping one Ho atom on the face of the metastable structure Si_{11}.

The lowest energy structure of Si_{13} (Fig. 2, 13a$_0$) is a distorted tri-capped pentagonal prism with C_{2v} symmetry. For $HoSi_{12}$, the lowest energy structure is obtained by substituting Ho atom for Si atom on the top of Si_{13} and it is not cage structure. Moreover, four lower energy isomers of $HoSi_{12}$ are created, and they are not cage structures, which is in line with the previous experimental result [27]. In addition, we have optimized a lot of initial geometries of $HoSi_{16}$ clusters and the results show that the fullerene like structure with Ho atom in the center of the silicon cage is not the lowest energy structure. Up to $n = 20$, a stable structure, a fullerene cage with Ho atom in the center, is a ground state structure with T_h symmetry, which is in good agreement with the experimental result in Ref. [26].

According to the results of the optimized lowest-energy structures of $HoSi_n$ clusters, we find that the Ho atom in the lowest energy configuration gradually moves from convex to the surface with n increasing from 1 to 12. Another obvious character is that the ground-state structures of $HoSi_n(n = 1 - 12)$ clusters are a replacement of Si atom in the most stable structures of pure Si_{n+1} clusters by Ho atom except $n = 7, 10$.

3.2 Relative stability of clusters

In order to study the relative stabilities of the most stable $HoSi_n$ clusters, it is significant to calculate the binding energy per atom ($E_b(n)$), the second difference in energy ($\Delta_2 E$) and the dissociation energy ($D(n)$). The binding energy per atom, the second difference in energy ($\Delta_2 E$) and the dissociation energy ($D(n)$) of $HoSi_n$ clusters can be defined as the following formulas:

$$E_b(n) = [E(\mathrm{Ho}) + nE(\mathrm{Si}) - E(\mathrm{HoSi}_n)]/n + 1 \quad (1)$$

$$\Delta_2 E(\mathrm{HoSi}_n) = E(\mathrm{HoSi}_{n+1}) + E(\mathrm{HoSi}_{n-1}) - 2E(\mathrm{HoSi}_n) \quad (2)$$

$$D(n, n-1) = E(\mathrm{HoSi}_{n-1}) + E(\mathrm{Si}) - E(\mathrm{HoSi}_n) \quad (3)$$

where E(Ho) and E(Si) are the single atom energies of Ho and Si, $E(\mathrm{HoSi}_n)$, $E(\mathrm{HoSi}_{n+1})$ and $E(\mathrm{HoSi}_{n-1})$ denote the total energies of the most stable $HoSi_n$, $HoSi_{n+1}$ and $HoSi_{n-1}$ clusters, respectively. Our calculation results are given in Figs. 3–5, respectively.

As shown in Fig. 3, the binding energy per atom of $HoSi_n$ and Si_n clusters generally increases as their sizes increase, which shows that these clusters can continue to getting energy during the growth process. Moreover, the average binding energy of $HoSi_n$ clusters is higher than that of pure Si_n clusters, implying that the doping of Ho atom can improve Si_n clusters' stability. We can also find that the average binding energy of $HoSi_n$ cluster have a large increase when the cluster size gets up to $n = 5$ and 8, which implies that $HoSi_5$ and $HoSi_8$ clusters are more stable than their neighbors.

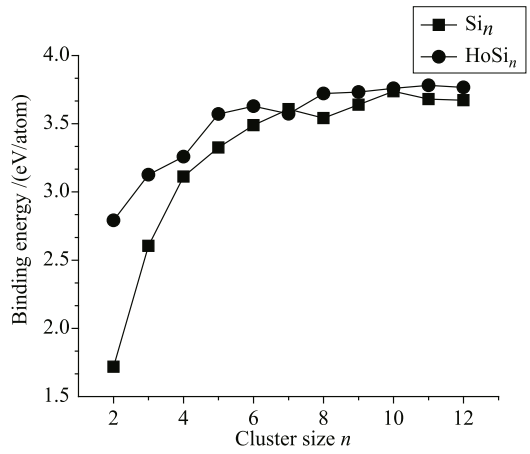

Fig. 3 The binding energies per atom of $HoSi_n$ and Si_n clusters.

As we know, the second-order difference in energy is a sensitive quantity which reflects the relative stability of clusters. From Fig. 4, we can see that the second-order difference in energy ($\Delta_2 E$) is a function of the cluster size. The maxima are found at $n = 2, 5, 8, 11$, indicating that these clusters own higher stability. However, the dissociation energy ($D(n)$) is also an accurate quantity to justify the stable magic number of $HoSi_n$ clusters.

Based on the calculated dissociation energies of $HoSi_n$ clusters shown in Fig. 5, four peaks on the dissociation energy curve are found at $n = 2, 5, 8$ and 11, reflecting that the calculated dissociation energies for $n = 2$, 5, 8 and 11 are larger than those of their neighbors. So we can conclude that $n = 2, 5, 8$ and 11 are the magic numbers of $HoSi_n$ clusters. And they have large abundances in mass spectroscopy relative to their neighbors, which is consistent with the conclusion of the second-order difference in energy that is shown in Fig. 4.

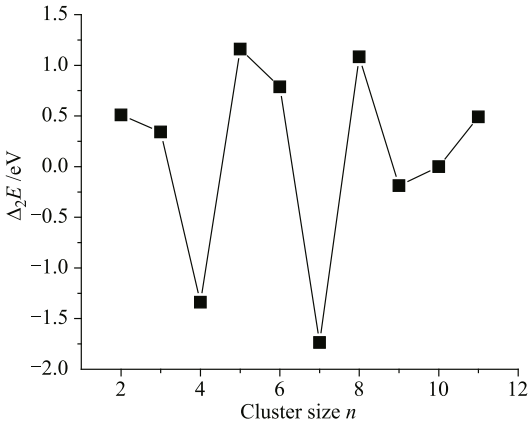

Fig. 4 The second difference in binding energy of $HoSi_n$ clusters.

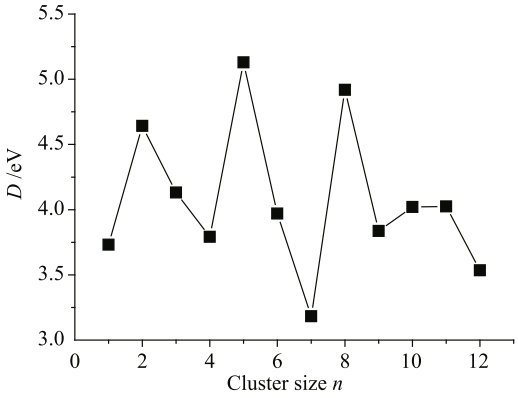

Fig. 5 The dissociation energy of $HoSi_n$ clusters.

3.3 Electronic and magnetic properties of clusters

The energy gap between the highest occupied molecular orbital (HOMO) and the lowest unoccupied molecular orbital (LUMO) reflects the electronic property of clusters. Figure 6 shows the energy gaps of the lowest energy structures of $HoSi_n$ clusters, together with the gaps of Si_n clusters to compare. As shown in Fig. 6, the energy gaps of the corresponding Si_n clusters are usually larger than those of the $HoSi_n$ clusters, but the gaps are close to each other at $n = 2, 3$ and 12. This indicates that the chemical activity of the clusters will be raised by the doping Ho atom in Si clusters. Moreover, the $HoSi_n$ clusters are in part metallic. In addition, two peaks with the size of $n = 5$ and 10 are shown in the curve, reflecting that the $HoSi_5$ and $HoSi_{10}$ clusters have larger HOMO–LUMO gaps and weaker chemical activities than their neighbors. Furthermore, the $HoSi_5$ cluster has the biggest E_{gap} value, indicating that the $HoSi_5$ cluster has the strongest chemical stability and $HoSi_5$ is a stable unit in chemical reaction.

The charge transfer and magnetic properties of $HoSi_n$ clusters are also calculated and the results are shown in

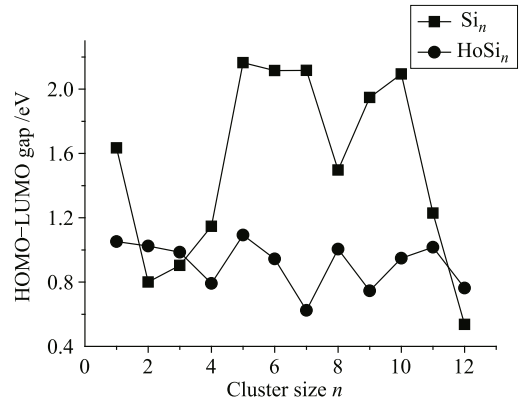

Fig. 6 The HOMO–LUMO gaps of $HoSi_n$ and Si_n clusters.

Fig. 7 and Fig. 8. Mulliken population analysis makes it clear that charges of $HoSi_n (n = 1–12)$ clusters often transfer from Ho atom to Si atom, indicating that Ho atom acts as electron donor. Moreover, the size-dependence of charge transfer exhibits three-step behavior, which can be clearly seen in Fig. 7. From HoSi to $HoSi_6$, the charge transfer of clusters begins to rise at a steady rate. Then from $HoSi_7$ to $HoSi_9$, it is like a parabola. Finally, charge transfer from $HoSi_{10}$ to $HoSi_{12}$

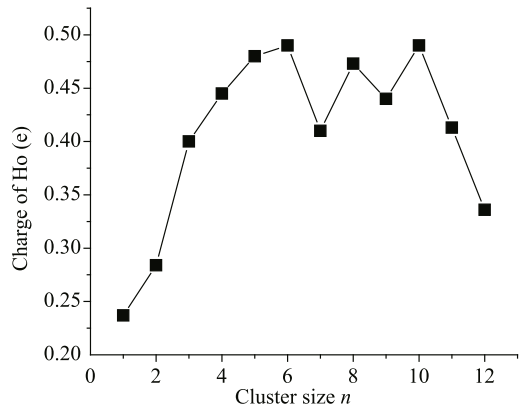

Fig. 7 Atomic charges of Ho atom of $HoSi_n$ clusters.

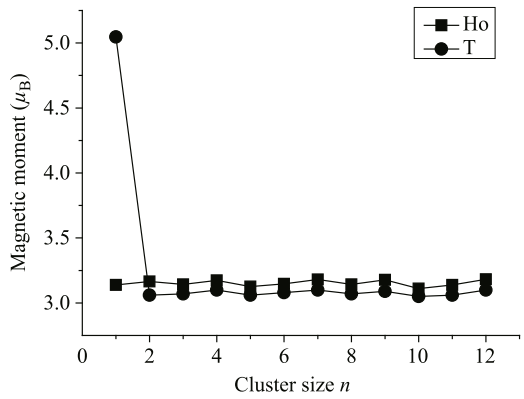

Fig. 8 Total magnetic moments (T) and magnetic moments (Ho) on Ho atom of $HoSi_n$ clusters.

decreases continuously. The alteration of charge transfer of $HoSi_n$ clusters is in accordance with the previous study on the $LaSi_n$ clusters [42].

The magnetic moment is another interesting property. In cluster size, there are even more properties distinct from those of molecular or bulk materials. On the basis of the optimized geometries, the magnetic properties of $HoSi_n$ clusters are acquired and the results are demonstrated in Fig. 8. The total magnetic moments of the $HoSi_n$ clusters almost keep a fixed value ($3.08\mu_B$) except when $n = 1$ and they largely lie on the Ho site. We can find little spin (about $0.06\mu_B$–$0.1\mu_B$) on the Si sites. Whereas, most of the local moments on Si atoms are discovered to arrange antiferromagnetically as opposed to the local moments of the Ho atom. Most importantly, the magnetic moment of Ho atom in $HoSi_n$ clusters is not quenched up to $HoSi_{12}$. It is distinct from $FeSi_n$, and $CrSi_n$ clusters. Their magnetic moments totally quench at n=10, 12, respectively [19, 43]. However, this is consistent with Bowen's speculation [26]. Namely, the magnetic moment of Ho atom in $HoSi_n$ clusters is not quenched. Furthermore, for larger $HoSi_{20}$ cluster (Fig. 2, 20a), a stable fullerene cage with complete encapsulation of the Ho atom into the center of the Si framework, the magnetic moment of Ho atom in $HoSi_{20}$ cluster is $3.26\mu_B$, indicating that the magnetic moment of Ho atom does not quench as well, which is similar with the results in Ref. [31] and Ref. [42].

A detailed analysis of the one-site atomic charges and local magnetic moments is conducted for a better understanding of the charge transfer and the magnetic properties of $HoSi_n$ clusters. Table 1 summarizes the charge and spin of $4f$, $5d$, $6s$ and $6p$ states of Ho atom in $HoSi_n$ clusters. The fact that the valence electron configuration of a free Ho atom is $4f^{11}6s^2$ is widely known. Nevertheless, Table 1 shows that the magnetic moment of the Ho atom is largely from $4f$ state and then the $5d$ state, while the $6s$ and $6p$ states contribute little to the magnetic moment of Ho atom. Bowen *et al.* [26] believe that even when Ho atom is enclosed by a Si cage, it can keep numerous portions of its magnetic moment due to the finite involvement of $4f$ electrons in bonding with its surroundings. Liu and co-workers [31] have studied magnetic fullerenes of silicon by RE metal encapsulation using DFT. The results show that the spin magnetic moment for $EuSi_{20}$ cluster is nearly $7\mu_B$, which mainly comes from the Eu $4f$ electrons. In the previous theoretical study [32], we have concluded that most of the $4f$ electrons of Eu atom in the $EuSi_{12}$ cluster have no interaction with the Si cage, and the $4f$ electrons of the Eu atom make contributions to the total magnetic moments' overwhelming majority. These findings demonstrate that the RE's f electrons in $RESi_n$ clusters have little interaction with their surroundings. So we reach the final conclusion that to a great degree the silicon cage has no interaction with the $4f$ electrons of Ho atom in the $HoSi_n$ clusters and they contribute largely to the total magnetic moments.

As for $HoSi_{20}$, a certain amount of electrons are lost by the $6s$ state of Ho atom and extra electrons are gained by $5d$, $6p$ states, which shows the existence of internal electron transfer among $6s$, $5d$ and $6p$ states in Ho atom. That is to say, a *spd* hybridization exists in Ho atom. In other words, Si cage seldom influences $4f$ electrons of Ho atom in fullerene cage $HoSi_{20}$ and the latter can probably retain large portions of their magnetic moments. Besides, the non-quench of magnetic moments might stem from *sp* hybridization in Si atom along with hybridization between Ho and Si atoms. Briefly, as for $HoSi_n$, $4f$ electrons are inactive with the silicon cluster which results in the non-quench of magnetic moments.

Table 1 The charge and magnetic moment of $4f, 5d, 6p$ and $6s$ states for Ho atom in $HoSi_n$ clusters.

	$4f$		$5d$		$6p$		$6s$	
n	Charge	Magnetic moment	Charge	Magnetic moment	Charge	Magnetic moment	Charge	Magnetic moment
1	10.956	3.036	0.385	0.309	0.151	0.059	1.276	0.263
2	10.933	3.051	0.680	0.064	0.180	0.009	0.931	0.049
3	10.951	3.036	0.578	0.043	0.179	0.013	0.896	0.060
4	10.937	3.048	0.771	0.065	0.229	0.016	0.626	0.053
5	10.950	3.033	0.677	0.050	0.193	0.013	0.705	0.041
6	10.933	3.045	0.792	0.059	0.238	0.018	0.548	0.038
7	10.903	3.076	0.744	0.061	0.269	0.019	0.681	0.038
8	10.928	3.049	0.854	0.062	0.253	0.020	0.496	0.030
9	10.893	3.088	0.931	0.063	0.301	0.020	0.460	0.024
10	10.944	3.033	0.710	0.049	0.245	0.016	0.617	0.027
11	10.914	3.063	0.732	0.048	0.305	0.020	0.642	0.024
12	10.880	3.099	0.736	0.049	0.326	0.023	0.702	0.027
20	10.737	3.180	2.399	0.049	0.488	0.043	0.712	0.003

4 Conclusions

In summary, we carry out a detailed investigation on the growth behavior, stabilities, electronic and magnetic properties of $HoSi_n$ clusters using DFT with GGA calculations. We find that for the lowest energy structures of $HoSi_n$ clusters, Ho atom always prefers locating on the surface site of the clusters, and they can be viewed as a replacement of Si atom in the most stable structures of pure Si_{n+1} clusters by Ho atom except $n = 7, 10$. According to the binding energy per atom ($E_b(n)$), the second difference in energy ($\Delta_2 E$) and $D(n)$, we conclude that the Ho atom doping enhances the stabilities of silicon clusters and $n = 2, 5, 8, 11$ are the magic numbers of $HoSi_n$ clusters. In addition, the Mulliken population analysis shows that the atomic charges of Ho atom of $HoSi_n$ clusters transfers from Ho atom to Si atoms up to $n = 12$. The total magnetic moments and the magnetic moments on Ho in the $HoSi_n (n = 1–12, 20)$ clusters do not quench because Ho $4f$ electrons to a large extent do not interact with the silicon cage.

Acknowledgements This work was supported by the National Natural Science Foundation of China under Grant No.11104231 and the Natural Science Foundation of Henan Province Education Department under Grant No. 2011B140008. We thank the institute of computational materials science, school of physics and electronics, Henan University for the calculation platform.

References

1. N. Uchida, T. Miyazaki, and T. Kanayama, Stabilization mechanism of Si_{12} cage clusters by encapsulation of a transition-metal atom: A density-functional theory study, *Phys. Rev. B*, 2006, 74(20): 205427
2. M. B. Torres, E. M. Fernández, and L. C. Balbás, Theoretical study of isoelectronic Si_nM clusters (M=Sc^-, Ti, V^+; $n = 14–18$), *Phys. Rev. B*, 2007, 75(20): 205425
3. J. Wang and J. G. Han, Geometries, stabilities, and electronic properties of different-sized $ZrSi_n (n = 1–16)$ clusters: A density-functional investigation, *J. Chem. Phys.*, 2005, 123(6): 064306
4. L. J. Guo, X. Liu, G. F. Zhao, and Y.H. Luo, Computational investigation of $TiSi_n (n = 2–15)$ clusters by the density-functional theory, *J. Chem. Phys.*, 2007, 126(23): 234704
5. S. M. Beck, Mixed metal–silicon clusters formed by chemical reaction in a supersonic molecular beam: Implications for reactions at the metal/silicon interface, *J. Chem. Phys.*, 1989, 90(11): 6306
6. S. M. Beck, Studies of silicon cluster–metal atom compound formation in a supersonic molecular beam, *J. Chem. Phys.*, 1987, 87(7): 4233
7. M. Ohara, K. Koyasu, A. Nakajima, and K. Kaya, Geometric and electronic structures of metal (M)-doped silicon clusters (M=Ti, Hf, Mo and W), *Chem. Phys. Lett.*, 2003, 371(3–4): 490
8. K. Koyasu, M. Akutsu, M. Mitsui, and A. Nakajima, Selective formation of MSi_{16} (M = Sc, Ti, and V), *J. Am. Chem. Soc.*, 2005, 127(14): 4998
9. J. B. Jaeger, T. D. Jaeger, and M. A. Duncan, Photodissociation of metal-silicon clusters: Encapsulated versus surface-bound metal, *J. Phys. Chem. A*, 2006, 110(30): 9310
10. H. Hiura, T. Miyazaki, and T. Kanayama, Formation of metal-encapsulating Si cage clusters., *Phys. Rev. Lett.*, 2001, 86(9): 1733
11. J. Lu and S. Nagase, Structural and electronic properties of metal-encapsulated silicon clusters in a large size range, *Phys. Rev. Lett.*, 2003, 90(11): 115506
12. P. Sen and L. Mitas, Electronic structure and ground states of transition metals encapsulated in a Si_{12} hexagonal prism cage, *Phys. Rev. B*, 2003, 68(15): 155404
13. J. U. Reveles and S. N. Khanna, Nearly-free-electron gas in a silicon cage, *Phys. Rev. B*, 2005, 72(16): 165413
14. J. U. Reveles and S. N. Khanna, Electronic counting rules for the stability of metal-silicon clusters, *Phys. Rev. B*, 2006, 74(3): 035435
15. N. Uchida, T. Miyazaki, and T. Kanyama, Stabilization mechanism of Si_{12} cage clusters by encapsulation of a transition-metal atom: A density-functional theory study, *Phys. Rev. B*, 2006, 74(20): 205427
16. F. C. Chuang, Y. Y. Hsieh, C. C. Hsu, and M. A. Albao, Geometries and stabilities of Ag-doped $Si_n (n = 1–13)$ clusters: A first-principles study, *J. Chem. Phys.*, 2007, 127(14): 144313
17. F. Hagelberg, C. Xiao, and Lester, Cagelike Si_{12} clusters with endohedral Cu, Mo, and W metal atom impurities, *Phys. Rev. B*, 2003, 67(3): 035426
18. V. Kumar and Y. Kawazoe, Magic behavior of $Si_{15}M$ and $Si_{16}M$ (M = Cr, Mo, and W) clusters, *Phys. Rev. B*, 2002, 65(7): 073404
19. L. Ma, J. Zhao, J. Wang, B. Wang, Q. Lu, and G. Wang, Growth behavior and magnetic properties of Si_nFe ($n = 2–14$) clusters, *Phys. Rev. B*, 2006, 73(12): 125439
20. J. G. Wang, J. J. Zhao, L. Ma, B. L. Wang, and G. H. Wang, Structure and magnetic properties of cobalt doped ($n = 2–14$) clusters, *Phys. Lett. A*, 2007, 367(4–5): 335
21. J. Wang, Q. M. Ma, Z. Xie, Y. Liu, and Y. C. Li, From Si_nNi to $Ni@Si_n$: An investigation of configurations and electronic structure, *Phys. Rev. B*, 2007, 76(3): 035406
22. T. Miyazaki, H. Hiura, and T. Kanayama, Topology and energetics of metal-encapsulating Si fullerenelike cage clusters, *Phys. Rev. B*, 2002, 66(12): 121403
23. M. Ohara, K. Miyajima, A. Pramann, A. Nakajima, and K. Kaya, Geometric and electronic structures of terbium-silicon mixed clusters ($TbSi_n$; $6 \leqslant n \leqslant 16$), *J. Phys. Chem. A*, 2002, 106(15): 3702

24. M. Ohara, K. Miyajima, A. Pramann, A. Nakajima, and K. Kaya, Geometric and electronic structures of terbium-silicon mixed clusters ($TbSi_n$; $6 \leqslant n \leqslant 16$), *J. Phys. Chem. A*, 2007, 111(42): 10884
25. A. Grubisic, H. P. Wang, Y. J. Ko, and K. H. Bowen, Photoelectron spectroscopy of europium-silicon cluster anions, $EuSi_n^-$ ($3 \leqslant n \leqslant 17$), *J. Chem. Phys.*, 2008, 129(5): 054302
26. A. Grubisic, Y. J. Ko, H. P. Wang, and K. H. Bowen, Photoelectron spectroscopy of Lanthanide-Silicon cluster anions $LnSi_n^-$ ($3 \leqslant n \leqslant 13$; Ln = Ho, Gd, Pr, Sm, Eu, Yb): Prospect for magnetic silicon-based clusters, *J. Am. Chem. Soc.*, 2009, 131(30): 10783
27. K. Koyasu, J. Atobe, S. Furuse, and A. Nakajima, Anion photoelectron spectroscopy of transition metal- and lanthanide metal-silicon clusters: MSi_n^- (n = 6–20), *J. Chem. Phys.*, 2008, 129(21): 214301
28. T. T. Cao, L. X. Zhao, X. J. Feng, Y. M. Lei, and Y. H. Luo, Structural and electronic properties of $LuSi_n$ (n = 1–12) clusters: A density functional theory investigation, *J. Mol. Struct. Theochem.*, 2009, 895(1–3): 148
29. R. N. Zhao, J. G. Han, J. T. Bai, F. Y. Liu, and L. S. Sheng, A relativistic density functional study of Si_n (n = 7–13) clusters with rare earth ytterbium impurity, *Chem. Phys.*, 2010, 372(1–3): 89
30. V. Kumar, A. K. Singh, and Y. Kawazoe, Charged and magnetic fullerenes of silicon by metal encapsulation: Predictions from *ab initio* calculations, *Phys. Rev. B*, 2006, 74(12): 125411
31. J. Wang, Y. Liu, and Y. C. Li, Magnetic silicon fullerence, *Phys. Chem. Chem. Phys.*, 2010, 12(37): 11428
32. G. F. Zhao, J. M. Sun, Y. Z. Gu, and Y. X. Wang, Density-functional study of structural, electronic, and magnetic properties of the $EuSi_n$ (n = 1–13) clusters, *J. Chem. Phys.*, 2009, 131(11): 114312
33. T. G. Liu, G. F. Zhao, and Y. X. Wang, Structural, electronic and magnetic properties of $GdSi_n$ (n = 1–17) clusters: A density functional study, *Phys. Lett. A*, 2011, 375(7): 1120
34. B. Delley, An all-electron numerical method for solving the local density functional for polyatomic molecules, *J. Chem. Phys.*, 1990, 92(1): 508
35. B. Delley, From molecules to solids with the $DMol^3$ approach, *J. Chem. Phys.*, 2000, 113(18): 7756
36. M. Dolg, U. Wedig, H. Stoll, and H. Preuss, Energy-adjusted *ab initio* pseudopotentials for the first row transition elements, *J. Chem. Phys.*, 1987, 86(2): 866
37. A. Bergner, M. Dolg, W. Küchle, H. Stoll, and H. Preuß, Ab initio energy-adjusted pseudopotentials for elements of groups 13–17, *Mol. Phys.*, 1993, 80(6): 1431
38. X. L. Zhu, X. C. Zeng, Y. A. Lei, and B. Pan, Structures and stability of medium silicon clusters. II. *Ab initio* molecular orbital calculations of Si_{12}–Si_{20}, *J. Chem. Phys.*, 2004, 120(19): 8985
39. A. A. Shvartsburg, B. Liu, M. F. Jarrold, and K. M. Ho, Modeling ionic mobilities by scattering on electronic density isosurfaces: Application to silicon cluster anions, *J. Chem. Phys.*, 2000, 112(10): 4517
40. C. Pouchan, D. Begue, and D. Y. Zhang, Between geometry, stability, and polarizability: Density functional theory studies of silicon clusters Si_n (n = 3–10), *J. Chem. Phys.*, 2004, 121(10): 4628
41. M. A. Belkhir, S. Mahtout, I. Belabbas, and M. Samah, Structure and electronic property of medium-sized silicon clusters, *Physica E*, 2006, 31(1): 86
42. T. T. Cao, X. J. Feng, L. X. Zhao, X. Liang, Y. M. Lei, and Y. H. Luo, Structure and magnetic properties of La-doped Si_n ($n = 1$–$12, 24$) clusters: a density functional theory investigation, *Eur. Phys. J. D*, 2008, 49(3): 343
43. S. N. Khanna, B. K. Rao, and P. Jena, Magic numbers in metallo-inorganic clusters: Chromium encapsulated in silicon cages, *Phys. Rev. Lett.*, 2002, 89(1): 016803